Environmental Science Advances

ROYAL SOCIETY OF CHEMISTRY

PAPER

View Article Online
View Journal | View Issue

Cite this: *Environ. Sci.: Adv.*, 2022, **1**, 356

A capture and inactivation system against pathogens in indoor air using copper nanoparticle decorated melamine sponge hybrid air filters†

Van Cam Thi Le, ‡[ab] Soyeong Yoon,‡[ac] Eunsil Kang,[ad] Mahshab Sheraz,[ab] Tae Uk Han,[e] Ali Anus, [ab] Hien Duy Mai,[ab] Sung-chan Choi[a] and Seungdo Kim *[abd]

The widespread transmission of coronavirus disease (COVID-19) poses an urgent need for air filter development to prevent pathogens from spreading in indoor spaces. This paper aims to introduce an *in situ* growth dip coating approach to demonstrate a simple and eco-friendly synthesis of copper nanoparticle (Cu NP) decorated melamine sponge (Cu/MS) air filters. The results showed that the Cu NPs tightly adhered to the melamine sponge (MS), and that their amount was controllable. Introducing increasing quantities of Cu NPs into the MS proportionally improved pathogen capture and inactivation efficiencies. The bare MS showed 94.54% capture efficiency, which was greatly improved up to 96.36% for Cu/MS (1.17 Cu wt%) and 100% for Cu/MS (5.69 Cu wt%) after 30 min. The capture performance of the Cu/MS air filter was stably maintained above 99% after multiple washing cycles due to the strong chemically grown Cu NPs on the MS carrier, indicating its reusability. Additionally, Cu/MS exhibited almost complete inactivation of *E. coli* (>99.99%) in saline, indicating that Cu NPs play a major role in the bacteria-killing function of Cu/MS. Taking advantage of the eco-friendliness, reusability and dual-functionality, the synthesized Cu/MS sponge filter would be an ideal candidate for the current and future pandemic situations.

Received 9th March 2022
Accepted 20th May 2022

DOI: 10.1039/d2va00041e

rsc.li/esadvances

Environmental significance

In the COVID-19 pandemic, the development of air filtration systems to capture and kill pathogens has become increasingly important to maintain the indoor air environment and reduce infection and mortal risk. This work presents a facile and eco-friendly synthesis of copper nanoparticles (Cu NPs) on melamine sponge (Cu/MS) as a reusable and dual-functional filter for pathogen capture and destruction in air. Quantitatively controllable and stable deposition of Cu NPs on MS leads to substantially enhanced pathogen capture and inactivation efficiencies. This study also provides insights into the design of a meaningful capture-and-disinfection air filter system to kill pathogens in a single-pass air flow.

1 Introduction

The coronavirus disease 2019 (COVID-19) pandemic has raised global concern regarding indoor air quality since people spend about 80% of their time in confined spaces.[1] Pathogen-containing aerosols are at the forefront of the COVID-19 pandemic's concern on the transmission of infectious diseases.[2,3] A recent study has clearly demonstrated that multiple individuals spending time in common indoor settings might pose a risk and facilitate virus transmission, indicating that this is a likely situation for efficient pathogen transmission.[4] To counter this escalating threat, the usage of air purifiers to mitigate the spread of infectious pathogens and regulate indoor air quality is highly desirable.[5]

Generally, air purification devices employed fibrous filters for capturing fine particulates due to a dense reticular meshwork. However, significant disadvantages of these fibrous filters are (1) high air resistance related to pressure drop, causing high energy consumption,[6] and (2) significant efficiency of pathogen removal.[7] In addition, it is reported that accumulation and proliferation of microbes leads to secondary airborne

[a]*Department of Environmental Sciences and Biotechnology, Hallym University, Chuncheon 24252, South Korea. E-mail: sdkim@hallym.ac.kr*

[b]*Nano-InnoTek Corporation, 123, Digital-ro 26-gil, Guro-gu, Seoul, South Korea*

[c]*Department of Environmental Engineering, Kangwon National University, Chuncheon 24341, South Korea*

[d]*Research Center for Climate Change and Energy (RCCCE), Hallym University, Chuncheon 24252, South Korea*

[e]*Environmental Resources Research Department, National Institute of Environmental Research, Hwangyeong-ro 42, Seo-gu, Incheon 22689, Republic of Korea*

† Electronic supplementary information (ESI) available. See https://doi.org/10.1039/d2va00041e

‡ Van Cam Thi Le and Soyeong Yoon contributed equally to the work and should be regarded as co-first authors.

contamination.[8] Eventually, the reduction of ventilation volume and the loss of filter life required additional maintenance and replacement costs. As a result, development of air filters with high capture and inactivation efficiency is required to improve indoor air quality and pathogen removal efficiency, and reduce the financial strain on air filters.[9]

To endow filter substrates with self-sterilizing anti-pathogen properties, incorporation of antimicrobial agents is needed.[10,11] Over the years, considerable research has been conducted to investigate antiviral activities of copper nanoparticles (Cu NPs).[12–14] Copper-based materials have been vigorously investigated for their rapid and high inactivation efficacy against pathogens such as the influenza virus (H1N1)[15] and coronaviruses such as severe acute respiratory syndrome coronavirus (SARS-CoV)[16] and human coronaviruses.[17] Consequently, copper was selected as the model antibacterial agent in this study due to its cost-effective and significant antiviral behavior. The critical issues are to find an appropriate substrate that is compatible with Cu NPs to achieve stable adhesion for extended reuse.

A key factor that should be taken into account is that Cu NPs in the form of powder can be a secondary particulate matter if the NPs are not tightly anchored on the filter substrate. Ultimately, melamine sponge (MS) was chosen for various reasons: (1) the spongy structure offers ideal filtration of polluted air flowing through sponge channels, thus minimizing pressure drop and energy consumption, (2) the highly porous structure can increase exposure of the antibacterial agents to the pathogens, and (3) the high density of amine functional groups is advantageous for nucleation and chemical adhesion of antimicrobial agents, and hence the filter would be reusable to some extent. Although some of the antibacterial capabilities of MS have been previously reported *via* antimicrobial agent coating,[18,19] there has been considerably less research on air treatment application, which is urgent in this pandemic.

Herein, a facile and eco-friendly development of a Cu NP encapsulated melamine sponge (Cu/MS) air filter is presented. The Cu/MS hybrid air filter exhibited outstanding performance for integrated capture and inactivation of pathogens present in aerosols. The Cu/MS (5.69 Cu wt%) filter served as a filtration medium with 100% filtration efficiency at a flow rate of 3 L min^{-1}, as well as >99.9% bactericidal activity toward *Escherichia coli* (*E. coli*) bacteria. Interestingly, the capture performance of airborne bacteria was maintained at above 99% after five washing cycles with water. The incorporation of Cu NPs is beneficial for the performance enhancement and the effect of incorporating different quantities of Cu NPs into the MS was evaluated in terms of capture and inactivation efficiencies. This work demonstrated an ideal approach for the simultaneous removal and inactivation of pathogens present in aerosols for air treatment especially in response to the ongoing COVID-19 pandemic.

2 Materials and methods

2.1. Materials

Melamine sponge (melamine–formaldehyde resin sponge) was bought from Dongsung Co., Ltd (South Korea). Copper(II) acetate monohydrate ($C_4H_8CuO_5$, 95%) and L-ascorbic acid ($C_6H_8O_6$, 99%) were purchased from TCI (America). Ethanol (C_2H_5OH, 95%) was provided by Daejung (South Korea). Distilled water was employed as the sole solvent for the Cu/MS synthesis. All the reagents were used as received without any purification and the stock solutions were freshly prepared before each reaction. *Escherichia coli* ATCC™ 25922™ (*E. coli*) was purchased from Thermo Fisher Scientific (South Korea) to investigate inactivation efficiencies for pathogens.

2.2. Fabrication of the Cu/MS hybrid air filter

Melamine sponge was used as a backbone substrate to fabricate the Cu/MS filter. The bare MS was sonicated for 30 min in ethanol for cleaning and dried under vacuum prior to the preparation of the Cu/MS. Subsequently, MS was cut into rectangular pieces of 40 × 40 × 80 mm^3 and immersed in 200 mL copper(II) acetate solution (concentration 9.12 mg mL^{-1}), followed by adding 10.56 g L-ascorbic acid. The mixture was vortexed and heated at 50 °C for 2 h. Afterwards, the Cu/MS was taken out and washed with distilled water to remove loosely bound particles and dried under vacuum. For comparison, Cu/MS with different Cu NP contents was also prepared under the same experimental conditions except this time 0.91 mg mL^{-1} copper(II) acetate solution and 1.056 g L-ascorbic acid were used.

2.3. Filtration test

The experiment design for evaluating the filtration ability of the Cu/MS filter was based on a previous report by Ramya *et al.*, with significant changes to the protocol.[20] Fig. 1a shows a schematic representation of the experiment setup, which includes an atomizer for generating bacterial aerosol. The *E. coli* suspension was sprayed with an air flow rate of 3 L min^{-1} into the plug flow reactor with a cross-section of 35 × 35 mm^2 and a length of 80 mm. The Cu/MS filter, measuring 35 × 35 × 10 mm^3, was incorporated into the reactor. The membrane was placed behind the Cu/MS filter to trap the bacteria in the outlet stream. The outlet stream from the module was passed into the bleach solution for safety purposes. At various time intervals of 30, 60, 90, 120, and 150 min, the membrane was removed and replaced. The removed membrane was rinsed in a beaker containing 10 mL phosphate-buffered saline (PBS). Afterwards, the bacterial solution (100 μL) from the beaker was inoculated on plate count agar (PCA) and incubated at 37 °C for 24 h. After incubation, the colonies were counted to determine the *E. coli* concentration. A blank test was carried out in the absence of Cu/MS to determine the number of bacterial colonies flowing through the empty module. Prior to the experiment, the optical density (OD) of the bacterial solution was adjusted to 1 using an ultraviolet-visible spectrometer at a wavelength of 600 nm in order to ensure that the concentration of bacteria passing through the different foam filters was consistent. The bare MS was tested under the same experimental conditions in addition to Cu/MS for comparison. Every test was repeated three times. Pathogen capture efficiency in air for Cu/MS sponge filters was calculated using eqn (1):

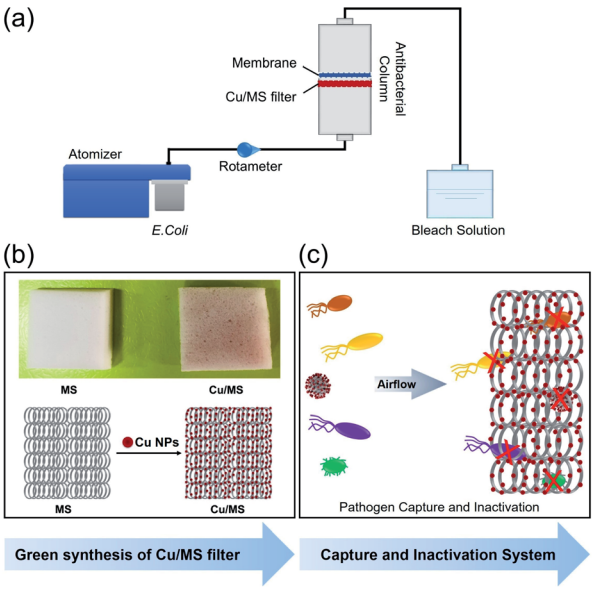

Fig. 1 (a) Schematic diagram of the experimental setup used in the pathogen capture tests; (b) digital camera images (top) and schematic illustration (bottom) of the copper decorated melamine sponge (Cu/MS) air filter fabrication process and (c) capture and inactivation air filter system-based Cu/MS.

$$\text{Efficiency} = \frac{C_0 - C}{C_0} \quad (1)$$

where C (CFU mL^{-1}) is the *E. coli* concentration in the presence of sponge filters and C_0 (CFU mL^{-1}) is the initial estimated bacterial concentration for each time point based on a blank test.

To check whether the filter can be reused, the pathogen capture test was performed after five washing cycles. Typically, the Cu/MS air filters were exposed to aerosol containing *E. coli* at a flow rate of 3 L min^{-1} for 150 min. Afterwards, the Cu/MS filters were fully washed with 20 mL distilled water under shaking at 300 rpm before being dried at 60 °C for 2 h. There were a series of experiments conducted for the pathogen capture tests during five cycles of the washing test.

2.4. Inactivation test

2.4.1. Inactivation kinetics. The plate count method was applied to determine the antibacterial performance of the Cu/MS filter. Cu/MS sponge air filters with size of 25 × 25 × 10 mm^3 were added to a batch reactor containing a mixture of 20 mL PBS and 0.2 mL *E. coli* solution (2.5 × 10^7 CFU mL^{-1}). The mixture was shaken at 230 rpm at 5, 10, 15, 30, 37 and 45 min, respectively. As the reaction proceeded, 100 μL of the bacterial solution was carefully pipetted out and plated in the PCA culture medium. These plates were incubated at 37 °C for 24 h, then the viable cell count was determined by the standard plate count method. The blank test was conducted under identical conditions in the absence of a Cu/MS filter. For comparison, the antibacterial performance of a bare MS was also assessed under the same conditions in addition to Cu/MS.

The inactivation kinetics of Cu/MS and bare MS filters were evaluated using the Chick–Watson equation, which is the empirical model for bacteria inactivation with a constant concentration of disinfectant, according to eqn (2):

$$\lg(C/C_0) = -k[\chi]^n t \quad (2)$$

where C_0 (CFU mL^{-1}) is the initial *E. coli* bacterial concentration and C (CFU mL^{-1}) is the bacterial concentration after varying time periods in the range of 5, 10, 15, 30, 37 and 45 min.

2.4.2. Optical density (OD_{600}) measurements. The optical densities of Cu/MS hybrid filters were measured at 600 nm. The Cu/MS filters were placed in a well grown bacteria *E. coli* suspension ($OD_{600} \sim 1.0$). The mixed suspension was kept in an incubator with continuous shaking at 230 rpm at different time periods of 0, 1, 2, 4, 6 and 9 h. At different time intervals, the optical density of the samples was measured at 600 nm to examine the bacterial growth after interaction with the sponges at different time periods. A graph of OD at 600 nm *versus* time was plotted to predict the growth of bacteria after interacting with increasing Cu NP content of Cu/MS samples.

2.4.3. Korea Conformity Laboratories standard method (KCL-FIR-1002:2021). The antibacterial activity of the Cu/MS filter was examined according to the Korea Conformity Laboratories standard method (KCL-FIR-1002:2021) procedure. This standard issued by Korea Conformity Laboratories (KCL) specifies the antibacterial performance of air cleaners installed in indoor places. Briefly, a Cu/MS filter with size of 50 × 50 × 10 mm^3 was added to a 100 mL Erlenmeyer flask containing 10 mL of Gram-negative *E. coli* suspensions (3.5 × 10^5 CFU mL^{-1}). The bacteria and antibacterial agents were mixed with a magnetic stirrer at room temperature for 3 minutes. Afterwards, the suspension inside the glass was carefully pipetted out and transferred to another sterilized tube. The suspension underwent a 10-fold serial dilution using saline solution and 100 μL of it was subsequently plated on agar. Finally, the plates were incubated at 37.1 ± 0.2 °C for 24 h and the viable cell count was then performed. The experiments were repeated three times and the assessed CFUs were normalized by the dilution factor and volume according to eqn (3):

$$\text{CFU mL}^{-1} = \frac{\text{no. of CFUs}}{(\text{dilution factor}) \times (\text{vol plated})} \quad (3)$$

The sterilization reduction rate (%) was calculated using the following equation (eqn (4)):

$$\text{Sterilization reduction rate (\%)} = \frac{[C_0 - C]}{C_0} \quad (4)$$

where C_0 (CFU mL^{-1}) is the initial *E. coli* bacterial concentration and C (CFU mL^{-1}) is the bacterial concentration in the presence of the Cu/MS filter after 24 h.

2.5. Characterization

The morphological structure of Cu/MS, MS and *E. coli* was imaged using scanning electron microscopy (SEM, Hitachi S-4800). An energy-dispersive X-ray analysis was carried out on

a JEOL JEM-2100F microscope. The functional groups and structure of Cu/MS as well as MS were analyzed using a Fourier transform infrared spectroscopy spectrometer (FT-IR, Thermo Scientific IN10) with a continuous scan in the range from 4000 to 400 cm^{-1}. X-ray diffraction (XRD) analysis was performed on a Rigaku Ultima IV diffractometer with focused-beam Cu K_α radiation ($K_\alpha = 1.541$ Å). The UV-vis spectra were obtained from a Shimadzu™ UVmini-1240 model spectrophotometer.

3 Results and discussion

3.1. *In situ* synthesis of Cu/MS

The fabrication procedures of the Cu/MS hybrid air filter are demonstrated in Fig. 1b and its usage in the pathogen capture and inactivation application is described in Fig. 1c. The Cu/MS was synthesized by the impregnation of MS with copper(II) acetate and subsequent treatment with L-ascorbic acid solution. The MS turned from light gray to light red, indicating the presence of Cu NPs. It was noticed that nontoxicity was considered as a significant aspect for the intended application. While there have been preliminary reports on the synthesis of Cu/MS,[21,22] the studies used hydrazine as a toxic reagent, which means that additional treatment for waste water emitted from the synthesis process will be required. Noteworthily, the synthesis of Cu/MS in this work was promising toward utilizing eco-friendly reducing agent L-ascorbic acid, which has not been previously described in the literature to the best of our knowledge.

To investigate the morphology of Cu NP growth on the bare MS, SEM images were used. As presented in Fig. 2a and S1,† the bare MS has a smooth surface and an interconnected 3D hole-like structure with a mean pore size of 135 ± 40 μm. After deposition of the Cu NPs, the spongy structure of Cu/MS was maintained, whereas the presence of the Cu NPs was observed on the backbone of the MS (Fig. 2b). The individual Cu NPs have pseudo-spherical topology with sizes of 430 ± 150 nm as seen in Fig. S2.† The composition of the Cu/MS hybrid sponge was mapped by SEM energy-dispersive spectroscopy (EDS) analysis (Fig. 2c). The presence of the Cu element confirmed that Cu NPs were incorporated and homogeneously distributed in the Cu/MS hybrid sponge. Additionally, the identified N, O and C elements were attributed to MS components, since MS consists of a formaldehyde–melamine copolymer.[23]

To better understand the mechanism of Cu/MS fabrication, FT-IR was carried out to determine the chemical bonds in the Cu/MS. Fig. 3a–c illustrate significant spectroscopic differences between bare MS and the treated Cu/MS sponges. The FT-IR spectrum of the MS shows the characteristic stretching vibration modes of N–H at 3337.7 cm^{-1}, while the vibration modes shift to a lower wavenumber of 3328.2 cm^{-1}, demonstrating that N–H formed the coordination bonds.[19] Moreover, the sharp absorption peak at 809.17 cm^{-1} observed for bare MS was shifted to 808.99 cm^{-1} for the Cu/MS. This peak was assigned to triazine ring bending,[24] and the shift could be related to changes in the aromaticity of the ring induced by the formation of the oximes.[25] A probable synthesis mechanism of the Cu/MS sponge filter is described in Fig. 3d. It was expected that the N-

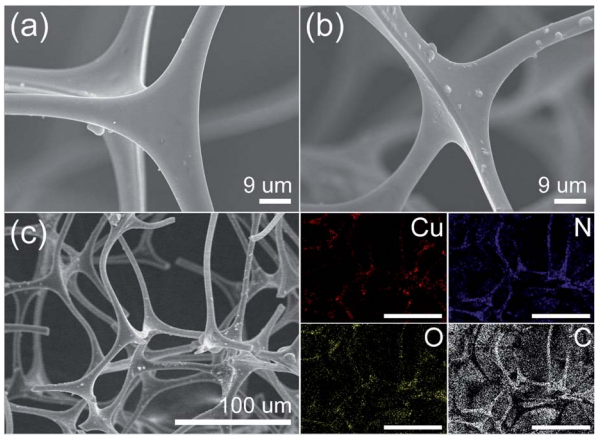

Fig. 2 Scanning electron microscopy (SEM) images of (a) melamine sponge (MS) and (b) Cu/MS (5.69 Cu wt%); (c) SEM and the corresponding elemental mapping of Cu/MS by energy-dispersive spectroscopy (EDS) analysis: Cu (red), N (blue), O (yellow), and C (gray).

pyridine and N–H groups of MS would form coordination bonds with the Cu^{2+} metal ion to cause chelation,[26,27] and subsequently be reduced by L-ascorbic acid. It should be noted that an alternative approach was to synthetically grow anti-pathogenic agents chemically bound to the surface of the carrier. In this work, a melamine sponge provided nucleation sites, which were beneficial for the growth of Cu NPs chemically bonded to the MS carrier.

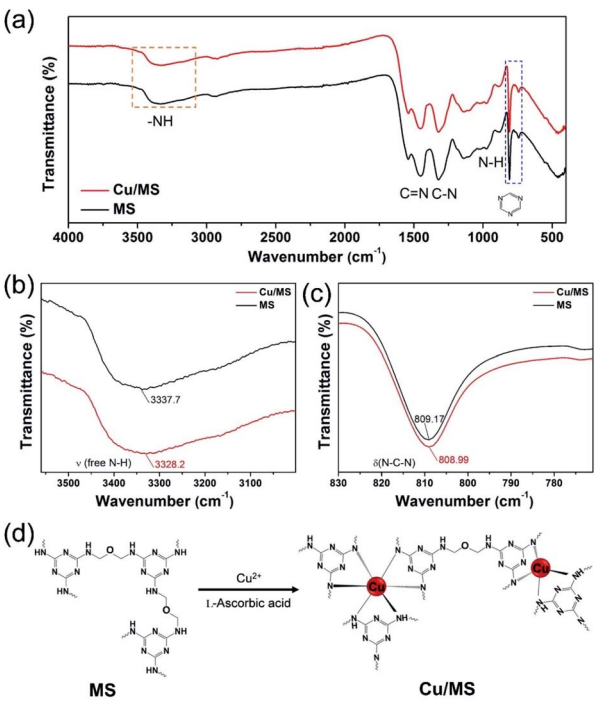

Fig. 3 (a) Fourier transform infrared spectroscopy (FT-IR) spectra of MS and Cu-CPP/MS (5.69 Cu wt%) sponge filters; (b and c) enlarged regions corresponding to the orange (b) and blue (c) boxes in image (a); (d) probable synthesis mechanism of the Cu/MS sponge filter.

It is noted that the treatment procedure allowed control of the Cu NP content on MS. For instance, the regulation of copper acetate concentration in the range of 0.91 to 9.12 mg mL^{-1} caused a rise in the amount of Cu NPs in the MS carrier. EDS analysis was used to determine the amount of copper that could be incorporated when it was transferred to the MS sponge (Fig. S3†). The Cu content of the Cu/MS sponge was measured to be 1.17% in the MS sponge treated in a 0.91 mg mL^{-1} $Cu(OAc)_2$ solution, while a higher Cu content (5.69%) on the sponge was obtained by increasing the $Cu(OAc)_2$ concentration (9.12 mg mL^{-1}). The pathogen-removal potential of the MS was indicated by the regulated copper nanoparticle coating formed on the MS surfaces.

3.2. Pathogen capture performance of the Cu/MS sponge filter

The spongy morphology with sinuous channels of MS allows air purifier and pathogen capture applications. The filtration performance of the Cu/MS sponge hybrid filters was evaluated using *E. coli* bioaerosol. The reason to choose *E. coli* bacterial aerosols was to target the respiratory droplet, since *E. coli* pathogens are commonly found in the indoor environment and are used widely in bioaerosol research. The pathogen aerosol passed through the column equipped with a Cu/MS sponge filter. It is worth noting that the membrane placed behind the Cu/MS sponge filter was used to trap the pathogen present in the outlet stream (Fig. 1a). As shown in Fig. S4,† the optical density (OD) of the *E. coli* solution was adjusted to $OD_{600nm} \sim 1.0$ using growth media in order to guarantee that the concentration of pathogen passing through the various sponge filters was consistent.

For the effectual capture of a pathogen, it was imperative to evaluate the capture performance of bare MS and Cu/MS with varying Cu NP contents. The Cu/MS was prepared with different loadings of Cu NPs (1.17 wt% and 5.69 wt%) in order to further elucidate the role of Cu NPs on MS. The number of viable bacterial colonies trapped by the membrane is shown in Fig. 4a. In principle, the large number of viable cells observed on the membrane is indicative of the lower capture performance toward pathogens, which results in a lower capture ability of the sponges. In the case of the blank, MS, and Cu/MS (1.17 Cu wt%), the number of *E. coli* colonies on the membrane increased proportionally with the exposure time, while in the case of Cu/MS (5.69 Cu wt%), no colonies were detected. The capture efficiencies were calculated and are displayed in Fig. 4b. After 30 min, the bare MS showed 94.54% capture efficiency, whereas Cu/MS (1.17 Cu wt%) was able to achieve a higher capture performance of 96.36%. Remarkably, Cu/MS (5.69 Cu wt%) exhibited the highest capture efficiency up to 100% during the same filtration time. Despite the fact that pathogen capture performance in the MS case decreased over time, Cu/MS (1.17 Cu wt%) still demonstrated significantly higher filtration performance than bare MS. It is worth noting that by increasing the amount of Cu NPs on MS (5.69 Cu wt%), a capture ability of up to 100% was achieved and maintained for 150 min. The results indicated that introducing increasing quantities of Cu NPs into the MS proportionally improved pathogen capture efficiency.

To explain the mechanism of filtration efficiency enhancement by introducing Cu NPs into the MS, SEM images of Cu/MS were recorded after the pathogen capture test was performed (Fig. 5). The SEM images of *E. coli* trapped in Cu/MS provided more details regarding the surface interaction between *E. coli*

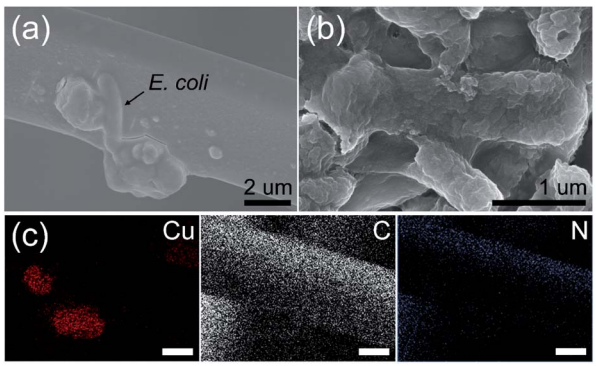

Fig. 5 (a) Scanning electron microscopy (SEM) image showing the surface interaction between *E. coli* and Cu NPs in Cu/MS, (b) SEM image showing a ruptured *E. coli* cell and (c) SEM and the corresponding elemental mapping showing the surface interaction between *E. coli* and Cu NPs in Cu/MS by EDS analysis: Cu (red), N (blue), O (yellow), and C (gray).

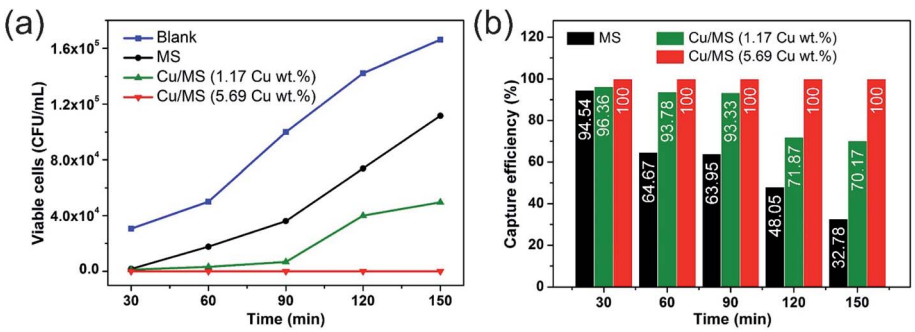

Fig. 4 (a) Bacterial growth for up to 150 min in the pathogen capture tests carried out with melamine sponge (MS), Cu/MS (1.17 Cu wt%) and Cu/MS (5.69 Cu wt%) sponge air filters and (b) a bar graph showing a comparison of the pathogen capture efficiencies for the MS, Cu/MS (1.17 Cu wt%) and Cu/MS (5.69 Cu wt%) sponge air filters.

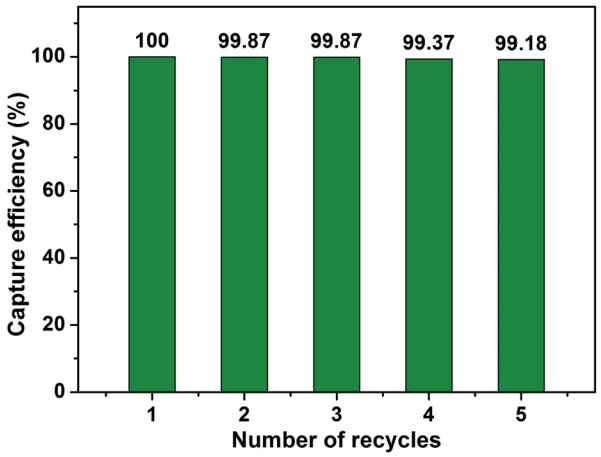

Fig. 6 Reusability of the Cu/MS (5.69 Cu wt%) air filter by monitoring the capture efficiency over five cleaning cycles.

and Cu NPs in Cu/MS. The SEM energy-dispersive spectroscopy (EDS) analysis confirmed the presence of *E. coli* bacteria with three-dimensional rod-shaped morphology (Fig. 5a and b), which were attached between Cu NPs within the Cu/MS hybrid sponge (Fig. 5c). The magnified SEM image shows that the Cu NPs were adsorbed on the *E. coli* surface in the form of clusters. When the bio-aerosol passed through the Cu/MS filter, the pathogen tended to come into contact with Cu NPs embedded in the MS skeleton. In particular, as a result of the high moisture condition in the aerosol, positively charged copper ions released from the copper particles tended to adhere to the negatively charged cell surface due to the electrostatic attraction between negatively charged bacterial cells and positively charged Cu NPs, thus damaging the outer and inner membranes of the bacterial cell.[20,28] Substantially, more bacteria were accumulated on the fiber surfaces when driven by electrostatic attraction, and dendrites of bacteria were formed.[29] As a result of the spongy morphology of MS incorporated with a controlled amount of Cu NPs as an anti-pathogenic agent, the pathogen capture ability may be controlled.

As an environmentally friendly and low-cost air filter, an ideal filter should have good reusability.[30–33] Therefore, the reusability of the Cu/MS sponge filter was evaluated under the cleaning method as follows: the Cu/MS filter was washed with distilled water under shaking at 300 rpm, followed by drying at 60 °C for 2 h. The capture performance of Cu/MS was examined over five cycles as illustrated in Fig. 6. During the reusability test, the capture performances were stably maintained above 99% after five runs. The excellent reusability of Cu/MS was attributed to the stable structure of the melamine sponge skeleton and strongly coordinated Cu NPs on the melamine sponge carrier.

3.3. Pathogen inactivation performance of the Cu/MS sponge filter

Antibacterial activity has become a prerequisite for an optimal air filter in order to lower the risk of pathogen infection and prevent microbial growth in filters. The incorporation of Cu NP antibacterial agents into the MS sponge has further enhanced the efficacy of the sponge since the pathogen was not only trapped but also inactivated. Herein, the inactivation experiments were conducted with an initial *E. coli* cell concentration of 2.5×10^7 colony-forming units (CFU) per mL. The inactivation tests were carried out with bare MS (without Cu NPs) and Cu/MS sponge filters with different Cu NP loading amounts (1.17 and 5.69 Cu wt%) to evaluate the effect of Cu NPs on

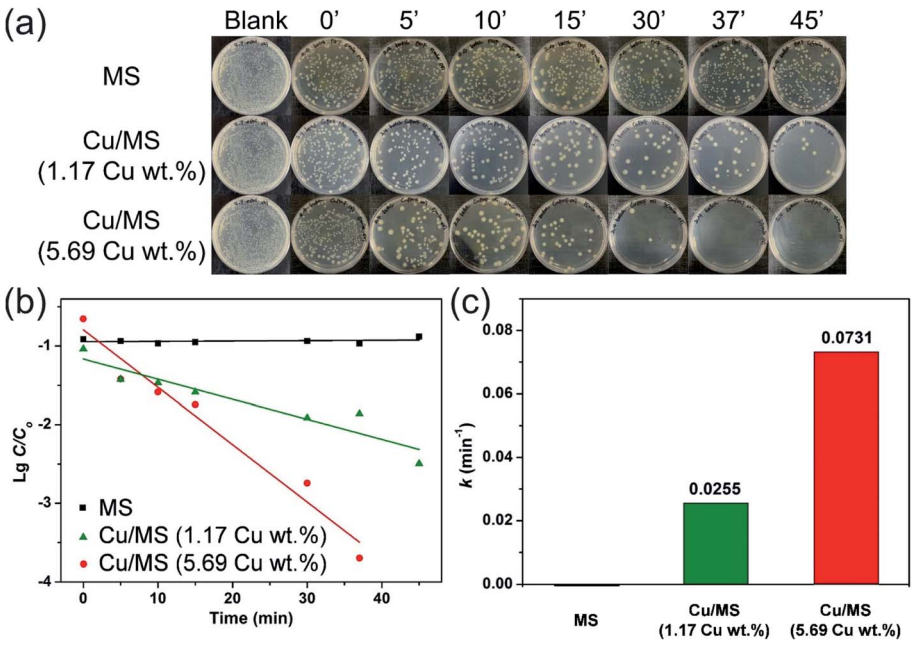

Fig. 7 (a) Digital images of cultivated *E. coli* colonies on agar culture plates, (b) inactivation kinetics on MS and Cu/MS with various Cu NP contents, and (c) the first-order disinfection rate on MS and Cu/MS with different Cu NP contents.

inactivation ability. When Cu/MS sponges were examined, the number of viable bacterial cells dropped significantly after 45 min; however, the number of living bacteria that survived on a bare MS filter remained unchanged (Fig. 7a). After 45 min, the inactivation efficiency against *E. coli* was negligible in the case of bare MS, which was further improved up to 99.7% when Cu/MS (1.17 Cu wt%) was used. Fig. 7b and c show the first-order inactivation rate of bare MS, which was significantly enhanced when Cu/MS (1.17 Cu wt%) was used, with a rate constant of 0.0255 min^{-1}. Cu/MS (5.69 Cu wt%) had a filter that reached 100% inactivation efficacy in 37 min, with an inactivation kinetic constant of 0.0731 min^{-1}.

The utilization of the Cu/MS hybrid sponge filter was also examined for water sanitation applications by placing the sponge samples in an *E. coli* bacterial suspension ($OD_{600} \sim 1.0$) (Fig. 8). The bare MS displayed poor antibacterial behavior and did not show bacterial growth inhibition, as presented by the increasing OD_{600} value for a time period of 9 h. In contrast, Cu/MS with a low Cu content (1.17 Cu wt%) hindered bacterial growth after 1 h, displaying constant OD_{600} values for a time period of 9 h. Interestingly, Cu/MS prepared with higher Cu content (5.69 wt%) inhibited bacterial growth instantly, showing the lowest OD_{600} value in comparison with contrasting materials MS and Cu/MS (1.17 Cu wt%).

In addition, we also carried out an antibacterial test under industrial standards. The antibacterial test was conducted according to the Korea Conformity Laboratories standard method (KCL-FIR-1002:2021). It was necessary to test the cellular viability after 24 h to ensure that no regrowth of the bacteria has occurred.[34,35] The antibacterial activity of the filter against *E. coli* was assessed through a comparison of the bacteria over the entire 24 h challenge period in the presence and absence of Cu/MS (Fig. 9 and Table 1). The Cu/MS filter displayed excellent bacterial reduction compared with blank samples after 24 h exposure. No growth of the viable cells was detected over 24 h. This assessment after 24 h was critical as

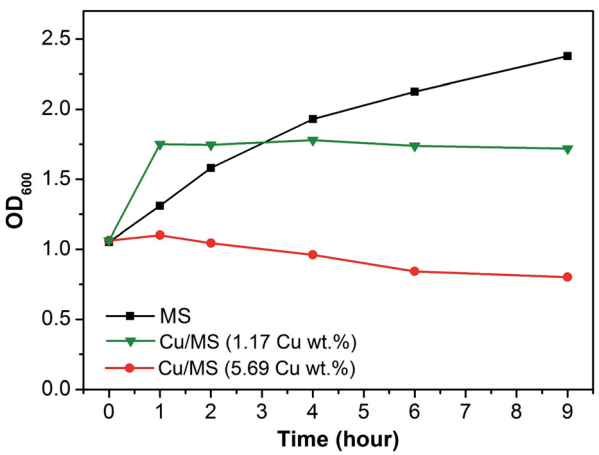

Fig. 8 Bacterial growth for up to 9 h of disinfection tests carried out with melamine sponge without (bare MS) and with varying Cu NP contents.

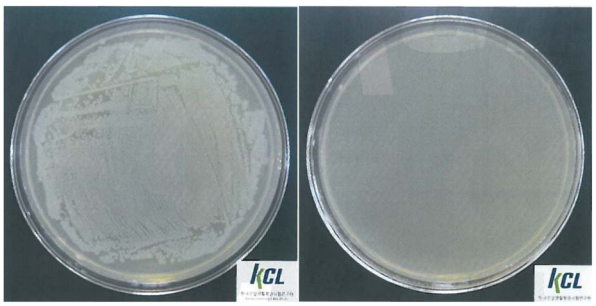

Fig. 9 (a) Digital images of cultivated *E. coli* colonies on agar culture plates of (a) blank and (b) Cu/MS (5.69 Cu wt%) filter after 24 h following the Korea Conformity Laboratories standard method (KCL-FIR-1002:2021).

Table 1 Antibacterial activity of the Cu/MS filter against *E. coli* after 24 h following the Korea Conformity Laboratories standard method (KCL-FIR-1002:2021)

Sample	Initial concentration (CFU mL^{-1})	Concentration after 24 h (CFU mL^{-1})	Reduction rate (%)
Blank	3.5×10^5	9.3×10^6	—
Cu/MS	3.5×10^5	<10	>99.9

reports have shown significant regrowth of bacteria after the initial efficacy was determined.[36]

The results suggest that the Cu/MS hybrid sponge filter was much more effective than the bare one in pathogen prevention and Cu NPs played a major role in the bacteria-killing function of Cu/MS. The antibacterial activity of copper nanoparticles was explained by two major mechanisms: (i) membrane depolarization, which is considered as the main mechanism. As a result of the high moisture content in the aerosol, positively charged copper ions were released from the copper particles, thus Cu ions were bound to negatively charged domains on the bacterial cell membrane, thereby reducing this potential difference causing membrane depolarization, which resulted in membrane rupture;[37,38] (ii) the genomic DNA undergoes degradation and the NPs may directly bind to domains in the DNA impairing its activity.[39]

Although there have been preliminary studies reporting copper as an antibacterial agent, the approach addressed in this work displayed the most promising method toward using Cu NPs associated with MS as a pathogen capture and inactivation system. Pinto *et al.* introduced Ag NPs grown on MS to test antibacterial performance,[19] but did not address the efficacy for air treatment, which is urgent in this COVID-19 pandemic. Chatzimitakos *et al.*[21] and Zhou *et al.*[22] successfully synthesized copper loaded on melamine sponge, but a toxic chemical (hydrazine) was used for the synthesis and they did not attempt to quantify the antibacterial application. However, no study has reported the pathogen capture and inactivation abilities using MS-based filters in an air phase as far as our literature search could ascertain. Although Ramya *et al.* developed air filter-based polyimide (PI) foam loaded Cu antimicrobial active metals, the

capture method lacked the quantification of different loadings of Cu NPs for validating the proposed capture mechanism to further elucidate the role of Cu NPs.[20] The fabrication of eco-friendly air filter-based MS incorporating controlled amounts of Cu NPs as an antimicrobial agent to prevent microbial growth and minimize pathogen spread is indeed the most promising avenue for novel biomaterials, making this work particularly powerful in its ability to capture and inactivate pathogens.

4 Conclusions

We demonstrated a facile, effective and eco-friendly synthesis for the growth of copper nanoparticles (Cu NPs) on melamine sponge (Cu/MS) as a reusable and dual-functional filter. The Cu/MS air filter showed excellent pathogen capture (100% capture efficacy) and inactivation behavior (>99.99% inactivation efficacy). Introducing increasing quantities of Cu NPs into the MS proportionally improved capture and inactivation efficiencies. Cu NPs play a major role as an antimicrobial agent to prevent microbial growth. This study provides valuable insights for the development of a capture and inactivation system to kill pathogens in a single-pass air flow.

Author contributions

Van Cam Thi Le: conceptualization, experiment design, analysis, methodology, figure design, writing – original draft preparation, review and editing. Soyeong Yoon: antimicrobial application experiment, draft preparation. Eunsil Kang: synthesis experiment. Mahshab Sheraz: review. Tae Uk Han: review and editing. Ali Anus: review. Hien Duy Mai: review and editing. Sung-chan Choi: antibacterial methodology. Seungdo Kim: funding acquisition, kinetic investigation, and supervision. All authors approved the final version of the manuscript.

Conflicts of interest

There are no conflicts to declare.

Acknowledgements

This work was financially supported by the Korea Ministry of Environment as Waste to Energy-Recycling Human Resource Development Project (YL-WE-21-001).

References

1 H. Qian, T. Miao, L. Liu, X. Zheng, D. Luo and Y. Li, Indoor transmission of SARS-CoV-2, *Indoor Air*, 2021, **31**, 639–645.
2 D. Vernez, S. Schwarz, J.-J. Sauvain, C. Petignat and G. Suarez, Probable aerosol transmission of SARS-CoV-2 in a poorly ventilated courtroom, *Indoor Air*, 2021, **31**, 1776–1785.
3 S. L. Miller, W. W. Nazaroff, J. L. Jimenez, A. Boerstra, G. Buonanno, S. J. Dancer, J. Kurnitski, L. C. Marr, L. Morawska and C. Noakes, Transmission of SARS-CoV-2 by inhalation of respiratory aerosol in the Skagit Valley Chorale superspreading event, *Indoor Air*, 2021, **31**, 314–323.
4 F. J. García de Abajo, R. J. Hernández, I. Kaminer, A. Meyerhans, J. Rosell-Llompart and T. Sanchez-Elsner, Back to normal: An old physics route to reduce SARS-CoV-2 transmission in indoor spaces, *ACS Nano*, 2020, **14**, 7704–7713.
5 E. S. Mousavi, N. Kananizadeh, R. A. Martinello and J. D. Sherman, COVID-19 outbreak and hospital air quality: A systematic review of evidence on air filtration and recirculation, *Environ. Sci. Technol.*, 2021, **55**, 4134–4147.
6 T. M. Korves, Y. M. Piceno, L. M. Tom, T. Z. DeSantis, B. W. Jones, G. L. Andersen and G. M. Hwang, Bacterial communities in commercial aircraft high-efficiency particulate air (HEPA) filters assessed by PhyloChip analysis, *Indoor Air*, 2013, **23**, 50–61.
7 P. Fermo, B. Artíñano, G. De Gennaro, A. M. Pantaleo, A. Parente, F. Battaglia, E. Colicino, G. Di Tanna, A. Goncalves da Silva Junior, I. G. Pereira, G. S. Garcia, L. M. Garcia Goncalves, V. Comite and A. Miani, Improving indoor air quality through an air purifier able to reduce aerosol particulate matter (PM) and volatile organic compounds (VOCs): Experimental results, *Environ. Res.*, 2021, **197**, 111131.
8 R. B. Simmons, D. L. Price, J. A. Noble, S. A. Crow and D. G. Ahearn, Fungal colonization of air filters from hospitals, *Am. Ind. Hyg. Assoc. J.*, 1997, **58**, 900–904.
9 V. C. T. Le, T. N. Thanh, E. Kang, S. Yoon, H. D. Mai, M. Sheraz, T. U. Han, J. An and S. Kim, Melamine sponge-based copper-organic framework (Cu-CPP) as a multi-functional filter for air purifiers, *Korean J. Chem. Eng.*, 2022, **38**, 1–12.
10 R. Medhi, P. Srinoi, N. Ngo, H.-V. Tran and T. R. Lee, Nanoparticle-based strategies to combat COVID-19, *ACS Appl. Nano Mater.*, 2020, **3**, 8557–8580.
11 V. C. T. Le, M. Sheraz, E. Kang, H. N. Ly, H. D. Mai, A. Anus and S. Kim, Alumina beads decorated copper-based coordination polymer particle filter for commercial indoor air cleaner, *Building and Environment*, 2022, **217**, 109012.
12 L. R. Jaidev, S. Kumar and K. Chatterjee, Multi-biofunctional polymer graphene composite for bone tissue regeneration that elutes copper ions to impart angiogenic, osteogenic and bactericidal properties, *Colloids Surf., B*, 2017, **159**, 293–302.
13 M. Hans, A. Erbe, S. Mathews, Y. Chen, M. Solioz and F. Mücklich, Role of copper oxides in contact killing of bacteria, *Langmuir*, 2013, **29**, 16160–16166.
14 A. Ananth, S. Dharaneedharan, M.-S. Heo and Y. S. Mok, Copper oxide nanomaterials: Synthesis, characterization and structure-specific antibacterial performance, *Chem. Eng. J.*, 2015, **262**, 179–188.
15 J. O. Noyce, H. Michels and C. W. Keevil, Inactivation of influenza a virus on copper *versus* stainless steel surfaces, *Appl. Environ. Microbiol.*, 2007, **73**, 2748–2750.
16 J. Han, L. Chen, S.-M. Duan, Q.-X. Yang, M. Yang, C. Gao, B.-Y. Zhang, H. He and X.-P. Dong, Efficient and quick inactivation of SARS coronavirus and other microbes

exposed to the surfaces of some metal catalysts, *Biomed. Environ. Sci.*, 2005, **18**, 176–180.

17 M. Hosseini, A. W. H. Chin, S. Behzadinasab, L. L. M. Poon and W. A. Ducker, Cupric oxide coating that rapidly reduces infection by SARS-CoV-2 *via* solids, *ACS Appl. Mater. Interfaces*, 2021, **13**, 5919–5928.

18 C.-H. Deng, J.-L. Gong, P. Zhang, G.-M. Zeng, B. Song and H.-Y. Liu, Preparation of melamine sponge decorated with silver nanoparticles-modified graphene for water disinfection, *J. Colloid Interface Sci.*, 2017, **488**, 26–38.

19 J. Pinto, D. Magrì, P. Valentini, F. Palazon, J. A. Heredia-Guerrero, S. Lauciello, S. Barroso-Solares, L. Ceseracciu, P. P. Pompa, A. Athanassiou and D. Fragouli, Antibacterial melamine foams decorated with *in situ* synthesized silver nanoparticles, *ACS Appl. Mater. Interfaces*, 2018, **10**, 16095–16104.

20 R. G., O. Camus, Y. M. J. Chew, B. Crittenden and S. Perera, Bactericidal–bacteriostatic foam filters for air treatment, *ACS Appl. Polym. Mater.*, 2020, **2**, 1569–1578.

21 T. G. Chatzimitakos and C. D. Stalikas, Melamine sponge decorated with copper sheets as a material with outstanding properties for microextraction of sulfonamides prior to their determination by high-performance liquid chromatography, *J. Chromatogr. A*, 2018, **1554**, 28–36.

22 H. Zhou, T. Zhang, X. Yue, Y. Peng, F. Qiu and D. Yang, Fabrication of flexible and superhydrophobic melamine sponge with aligned copper nanoparticle coating for self-cleaning and dual thermal management properties, *Ind. Eng. Chem. Res.*, 2019, **58**, 4844–4852.

23 Y. Feng and J. Yao, Design of melamine sponge-based three-dimensional porous materials toward applications, *Ind. Eng. Chem. Res.*, 2018, **57**, 7322–7330.

24 H. Gao, P. Sun, Y. Zhang, X. Zeng, D. Wang, Y. Zhang, W. Wang and J. Wu, A two-step hydrophobic fabrication of melamine sponge for oil absorption and oil/water separation, *Surf. Coat. Technol.*, 2018, **339**, 147–154.

25 D. J. Merline, S. Vukusic and A. A. Abdala, Melamine formaldehyde: curing studies and reaction mechanism, *Polym. J.*, 2013, **45**, 413–419.

26 Y. Ding, W. Xu, Y. Yu, H. Hou and Z. Zhu, One-step preparation of highly hydrophobic and oleophilic melamine sponges *via* metal-ion-induced wettability transition, *ACS Appl. Mater. Interfaces*, 2018, **10**, 6652–6660.

27 P. Kallenbach, E. Bayat, M. Ströbele, C. P. Romao and H.-J. Meyer, Tricopper melaminate, a metal–organic framework containing dehydrogenated melamine and Cu–Cu bonding, *Inorg. Chem.*, 2021, **60**, 16303–16307.

28 W. Shin, H. S. Han, N. T. K. Le, K. Kang and H. Jang, Antibacterial nanoparticles: enhanced antibacterial efficiency of coral-like crystalline rhodium nanoplates, *RSC Adv.*, 2019, **9**, 6241–6244.

29 D. Y. Choi, K. J. Heo, J. Kang, E. J. An, S.-H. Jung, B. U. Lee, H. M. Lee and J. H. Jung, Washable antimicrobial polyester/aluminum air filter with a high capture efficiency and low pressure drop, *J. Hazard. Mater.*, 2018, **351**, 29–37.

30 S. Jeong, H. Cho, S. Han, P. Won, H. Lee, S. Hong, J. Yeo, J. Kwon and S. H. Ko, High efficiency, transparent, reusable, and active PM2.5 filters by hierarchical Ag nanowire percolation network, *Nano Lett.*, 2017, **17**, 4339–4346.

31 S. Ullah, A. Ullah, J. Lee, Y. Jeong, M. Hashmi, C. Zhu, K. I. Joo, H. J. Cha and I. S. Kim, Reusability comparison of melt-blown *vs.* nanofiber face mask filters for use in the coronavirus pandemic, *ACS Appl. Nano Mater.*, 2020, **3**, 7231–7241.

32 N. El-Atab, N. Qaiser, H. Badghaish, S. F. Shaikh and M. M. Hussain, Flexible nanoporous template for the design and development of reusable anti-COVID-19 hydrophobic face masks, *ACS Nano*, 2020, **14**, 7659–7665.

33 L. Liao, W. Xiao, M. Zhao, X. Yu, H. Wang, Q. Wang, S. Chu and Y. Cui, Can N95 respirators be reused after disinfection? How many times?, *ACS Nano*, 2020, **14**, 6348–6356.

34 K. A. Poelstra, N. A. Barekzi, A. M. Rediske, A. G. Felts, J. B. Slunt and D. W. Grainger, Prophylactic treatment of gram-positive and gram-negative abdominal implant infections using locally delivered polyclonal antibodies, *J. Mater. Chem. B*, 2002, **60**, 206–215.

35 H. N. Rubin, B. H. Neufeld and M. M. Reynolds, Surface-anchored metal–organic framework–cotton material for tunable antibacterial copper delivery, *ACS Appl. Mater. Interfaces*, 2018, **10**, 15189–15199.

36 A. Pegalajar-Jurado, C. D. Easton, K. E. Styan and S. L. McArthur, Antibacterial activity studies of plasma polymerised cineole films, *J. Mater. Chem. B*, 2014, **2**, 4993–5002.

37 L. Fang, P. Cai, W. Chen, W. Liang, Z. Hong and Q. Huang, Impact of cell wall structure on the behavior of bacterial cells in the binding of copper and cadmium, *Colloids Surf., A*, 2009, **347**, 50–55.

38 M. Vincent, P. Hartemann and M. Engels-Deutsch, Antimicrobial applications of copper, *Int. J. Hyg. Environ. Health*, 2016, **219**, 585–591.

39 D. Mitra, E.-T. Kang and K. G. Neoh, Antimicrobial copper-based materials and coatings: Potential multifaceted biomedical applications, *ACS Appl. Mater. Interfaces*, 2020, **12**, 21159–21182.